06 Jun 2018

Modeling and Simulation of Mass Flow of Steel Plate/Slab during Hot Rolling

X. Wang

S. Ganguly

K. Chandrashekhara
Missouri University of Science and Technology, chandra@mst.edu

Mario F. Buchely
Missouri University of Science and Technology, buchelym@mst.edu

et. al. For a complete list of authors, see https://scholarsmine.mst.edu/mec_aereng_facwork/4464

Recommended Citation

X. Wang and S. Ganguly and K. Chandrashekhara and M. F. Buchely and S. N. Lekakh and D. C. Van Aken and R. J. O'Malley and D. Bai and Y. Wang and T. Natarajan, "Modeling and Simulation of Mass Flow of Steel Plate/Slab during Hot Rolling," *Proceedings of the AIST 2nd International Symposium on the Recent Developments in Plate Steels (2018, Orlando, FL)*, Association for Iron & Steel Technology (AIST), Jun 2018.

2nd International Symposium on the Recent Developments in Plate Steels, June 3-6, 2018, Orlando, FL

Modeling and Simulation of Mass Flow of Steel Plate/Slab during Hot Rolling

X. Wang, S. Ganguly, K. Chandrashekhara, M. F. Buchely, S. N. Lekakh, D. C. Van Aken and R. J. O'Malley
Missouri University of Science and Technology, Rolla, MO 65409

D. Bai and Y. Wang
SSAB Americas, Muscatine, IA 52761

T. T. Natarajan
United States Steel Corporation, Munhall, PA 15120

Keywords: Hot rolling, finite element, mass flow, plate, slab

ABSTRACT

The ability to predict mass flow behavior during hot rolling is essential to product quality. In this study, viscoplastic models of the steels from SSAB and U.S. Steel were developed based on experimental stress-strain curves. A three-dimensional nonlinear finite element model was built to simulate a reverse plate hot rolling and a hot strip rolling process. For plate rolling, a seven pass schedule was simulated. The plastic strain distributions during rolling were investigated. The results show that the surface of the plate has larger plastic strain than the center. In the case of hot strip rolling, the simulation predicts that material flows from the sides to the top and bottom surfaces during edging. The top and bottom surfaces were then rolled flat. Details of the material flow and strain distributions during edging and rolling are presented in this paper.

INTRODUCTION

Hot rolling is an important deformation process in steel manufacturing. In hot rolling, the rolls are subjected to cyclic thermal and mechanical loadings. Thermo-mechanical stress and strain variations occur due to rolling force/pressure imparted by roll contact, and non-uniform temperature distribution. The quality of final product is highly dependent on the thermo-mechanical deformation and mass flow behavior during hot rolling. In plate hot rolling, a plate goes back and forth between one pair of rollers. Each pass contributes a small deformation to the plate. In hot strip rolling, multiple stands and edgers are used. Edgers are used to mainly control the spread and squeeze of the strip width. Investigation of plastic strain and mass flow behavior of steel is important for understanding final product quality and performance. However, it is difficult and costly to investigate mass flow behavior using plant trials. Finite element methods provide an effective and economic way to model these thermomechanical processes and the associated mass flow behavior.

The objective of the current work is to utilize the finite element method to simulate hot rolling of steel. A finite element model was developed to study the plastic strain and mass flow during hot rolling. Kim and Im [1] used a finite element methodology to analyze non-isothermal hot rolling where the development of temperature gradient during rolling was examined. Duan and Sheppard [2] predicted the thermomechanical properties of aluminum alloys during hot rolling. Ding et al. [3] simulated microstructure evolution during hot rolling of AM50 Mg alloy and showed that temperature had a more significant effect on recrystallization than roll speed. Mei et al. [4] developed a finite element model to simulate strip temperature during hot rolling and Benasciutti et al. [5] predicted thermal stress development during hot rolling.

Various material models have been developed to describe mass flow behavior during hot rolling. The Johnson-Cook model [6] is one of the most widely used phenomenological constitutive model considering effects of strain hardening, strain rate hardening and temperature softening. Another widely used model, the Zerilli–Armstrong model [7], is based on dislocation mechanisms including models for BCC and FCC structures. The Shida model [8] provides an empirical constitutive model considering the effect of carbon content, strain, strain rate and temperature on plain carbon steels.

In the current study, three-dimensional nonlinear finite element models were built to simulate the plate hot rolling at SSAB Americas and strip hot rolling at U.S. Steel. Nonlinear material models were developed for the slab and the plate. For plate hot rolling, a single pair of rollers were used to deform the steel plate. The plate moved back and forth between the rollers until the desired shape was obtained. For slab hot rolling, the steel slab was rolled through a series of mill stands in a continuous and unidirectional process, which included both rollers and edgers. Mass flow and plastic strains during the hot rolling were predicted by finite element method and the simulation results are compared.

NONLINEAR MATERIAL MODEL

In the current study, two steel grades received from SSAB Americas and U. S. Steel were investigated. Hot tension tests were conducted to obtain the thermomechanical properties of these steels. The material properties were obtained at multiple temperatures (900°C, 1000°C, 1100°C, and 1200°C) and strain rates ($1s^{-1}$, $10s^{-1}$ and $20s^{-1}$) for SSAB steel grade. Similar tests were conducted on the US Steel samples at various temperatures (900°C, 1000°C, 1100°C, and 1200°C) and strain rates ($1s^{-1}$, $5s^{-1}$, $15s^{-1}$, and $30s^{-1}$). The results obtained from these tests were used to obtain the material constants needed to define the nonlinear material behavior. Representative stress-strain curves of the two steel grades are shown in Figure 1.

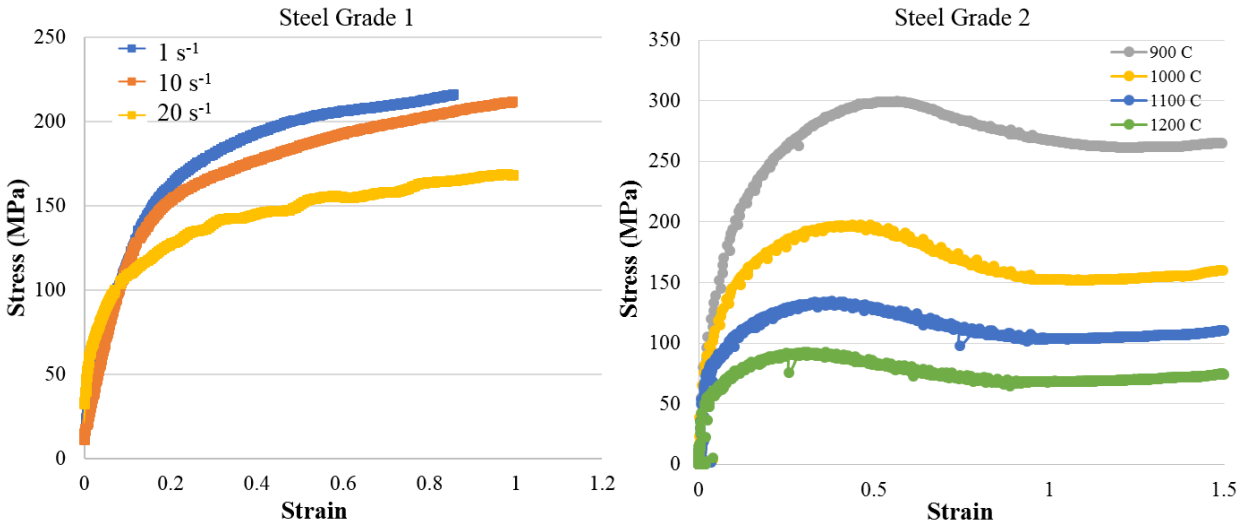

Figure 1. Examples of stress-strain curves of the steels from SSAB (Grade 1) and U. S. Steel (Grade 2)

It was essential to select a strain and temperature dependent constitutive material model to describe the metal mass flow behavior during hot rolling process. Among constitutive material models, Johnson-Cook model has been widely used and has successfully described material mass flow behavior, strain hardening and thermal softening during hot deformation [9]. The form of Johnson-Cook model used in this study is presented in Eq. 1

$$\sigma = (A + B\varepsilon^{n})(1 + C\ln\dot{\varepsilon}^{*})(1 - T^{*m}) \tag{1}$$

where σ is equivalent flow stress, ε is equivalent plastic strain, $\dot{\varepsilon}^{*}$ is dimensionless strain rate which is $\dot{\varepsilon}^{*} = \dot{\varepsilon}/\dot{\varepsilon}_0$, $\dot{\varepsilon}$ is strain rate and $\dot{\varepsilon}_0$ is reference strain rate, T^{*} is homologous temperature which is $T^{*} = (T - T_r)/(T_m - T_r)$, T_r is reference temperature and T_m is metal melting temperature. *A*, *B*, *C*, *m* and *n* are material parameters. The constants *A*, *B* and *n* describe the strain hardening effect, C describes the strain rate effect, and m describes the thermal softening effect of the material.
A non-linear regression method was considered in this work to obtain fitness function *X* that represented each set of the material constants (Eq. 2). The objective of the regression was to minimize the sum of squares error between experimental data and prediction of Johnson-Cook model.

$$\min f(x) = min\sum_{i=1}^{N}(\sigma_i^{exp} - \sigma_i^{JC}(X))^2 \tag{2}$$
$$X = [A, B, n, C, m]$$

where *N* is number of experimental data points, σ_i^{exp} is experimental stress value at data point i, and $\sigma_i^{JC}(X)$ is Johnson-Cook model prediction based on constant set *X* at data point *i*. Constants determined for the two steel grades are shown in Table 1

[10].

Table 1. Johnson-Cook constants

	A (MPa)	B (MPa)	C	n	m	$\dot{\varepsilon}_0$ (s^{-1})	T_r (°C)
Grade 1	20	155	0.136	0.340	0.912	1	1000
Grade 2	40	343	0.074	0.364	0.634	1	1000

FINITE ELEMENT MODEL

Nonlinear three-dimensional finite element models were developed to simulate both plate and strip hot rolling. Three-dimensional formulation of the dynamic response to deformation can be described by Eq. 3.

$$[M^e]\{\ddot{\Delta}^e\} + [K^e]\{\Delta^e\} = \{F^e\} + \{F^t\} \tag{3}$$

where $[M^e]$ and $[K^e]$ are mass matrix and the stiffness matrix respectively. $\{\Delta^e\}$ and $\{\ddot{\Delta}^e\}$ are displacement and acceleration respectively. $\{F^e\}$ is the loading vector and $\{F^t\}$ is the thermal loading. The commercial software ABAQUS 6.10 Dynamic-Explicit solver was used to build finite element models. An explicit central-difference method was used for time integration:

$$\{\ddot{\Delta}^e\}_{(i)} = [M^e]^{-1}(\{F^e\}_{(i)} - \{I^e\}_{(i)}) \tag{4}$$

$$\{\dot{\Delta}^e\}_{(i+1/2)} = \{\dot{\Delta}^e\}_{(i-1/2)} + \frac{\Delta t_{i+1}+\Delta t_i}{2}\{\ddot{\Delta}^e\}_{(i)} \tag{5}$$

$$\{\Delta^e\}_{(i+1)} = \{\Delta^e\}_{(i)} + \Delta t_{(i+1)}\{\dot{\Delta}^e\}_{(i+1/2)} \tag{6}$$

where $\{I^e\}_{(i)}$ means internal force vector and subscript i represents increment step number. Hard contact was assumed between the rigid rollers and the deformable work roll. Since shear forces are also transmitted along the surface of contact, a value of 0.25 was assumed for the rolling coefficient of friction to model the frictional forces between the contacted surfaces.
A three-dimensional finite element model was built for the SSAB plate rolling (Figure 2). The slab used for this product was 6 inch thick, 97 inch wide, and 118.11 inch long. The roller diameter was 35.6 inch and the length was 161.604 inch. The entering speed of plate was 5.36 ft/s, and the rotation speed of roller was 3.94 rad/s. Element C3D8RT was used to mesh the plate whereas R3D4 was used to mesh the rigid roller. The initial temperature of plate was maintained at 1155 °C, and the roller temperature was kept at 150 °C. Convection and radiation of hot plate was modeled to represent the decreasing temperature of plate during hot rolling. The film coefficient is set as 135 W/m^2℃, and emissivity is set as 0.8 W/m℃.

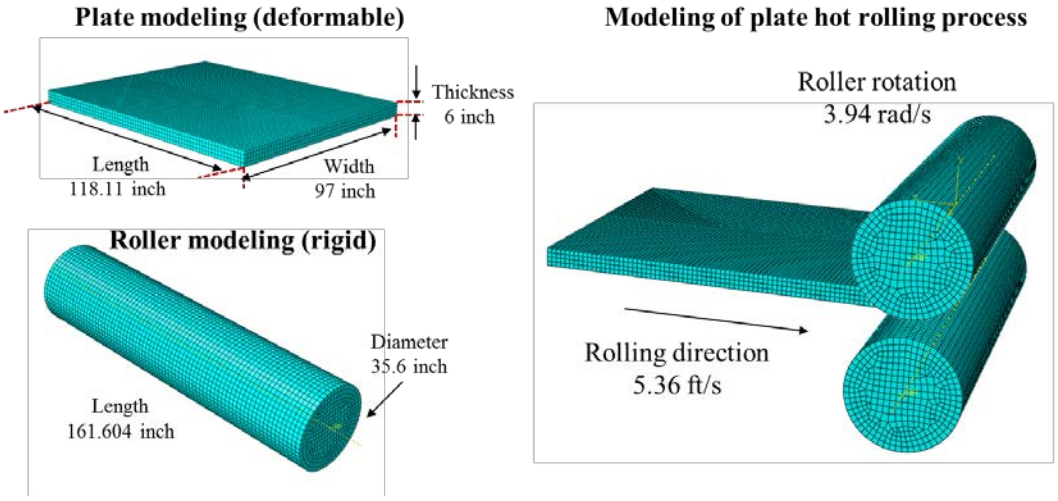

Figure 2. Schematic of the plate hot rolling

Another three-dimensional finite element model was built to simulate the U. S. Steel hot strip rolling (Figure 3). The slab used for this product was 9.1 inch thick, and 46.25 inch wide. Typical length of slab at U. S. Steel is 240 inch to 360 inch. To save computational time, the modeled length of slab is 118.11 inch. Five pairs of rollers from R1 to R5 and four pairs of edgers from E1 to E4 were modeled. The rollers and edgers were modeled as rigid bodies, while the deformation characteristics of the slab was modeled using the Johnson-Cook constitutive model. The initial temperature of the slab was maintained at 1200 °C, and the roller and edger temperatures were kept at 150 °C. Similarly, convection and radiation is considered in this model to simulate the temperature variation of slab during hot rolling. The coefficients of convection and radiation are set as 135 W/m^2℃ and 0.8 W/m℃ repectively.

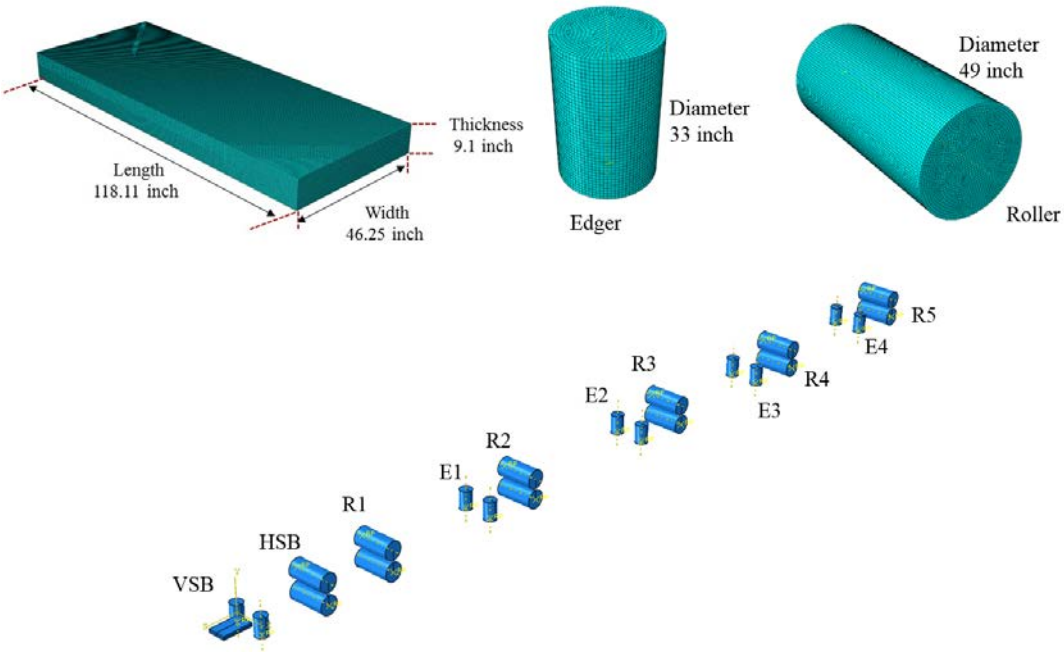

Figure 3. Schematic of the US Steel hot strip rolling sequence

RESULTS AND DISCUSSION

Simulation results of plate hot rolling

The plate hot rolling employed by SSAB Americas is a 4-high reversing rolling mill. The detailed pass schedule is shown in Table 2. The initial thickness of plate is 6 inch, and the final thickness after pass 7 is 3 inch. The 3 inch deformation is not equally distributed on the seven passes. The initial passes (P1 and P2) and ending passes (P6 and P7) have smaller deformation with around 5% reduction, while the middle passes (P3-P5) have larger deformation with around 10-15% reduction.

Table 2. The rolling schedule of plate hot rolling

Pass	Mill speed (fpm)	Roll time (s)	Thickness (inch)	Reduction %
1	349	4.1	5.642	5.97
2	402	4.1	5.316	5.78
3	504	4.3	4.603	13.41
4	415	5.2	3.936	14.49
5	587	5.3	3.518	10.62
6	500	6.0	3.287	6.57
7	299	8.2	3.088	6.05

The simulation result of the first pass P1 is shown in Figure 4. A comparison of plastic strain distribution between the surface and the center of the plate is shown in a symmetric plot. At P1, the roll gap is 5.642 inch and the reduction is 5.97%, introducing a relatively small deformation to the plate. The plastic strain at the plate surface is around 0.1, while the plastic strain at the plate mid-thickness is around 0.05. Due to small reduction and uneven temperature distribution, the surface gets more plastic

strain and this strain gradually decreases towards the plate mid-thickness. The maximum deformation at the plate surface is around 4.18 mm, and the deformation near the plate mid-thickness is only 0.35 mm since deformation barely penetrates to the plate mid-thickness for the given deformation condition.

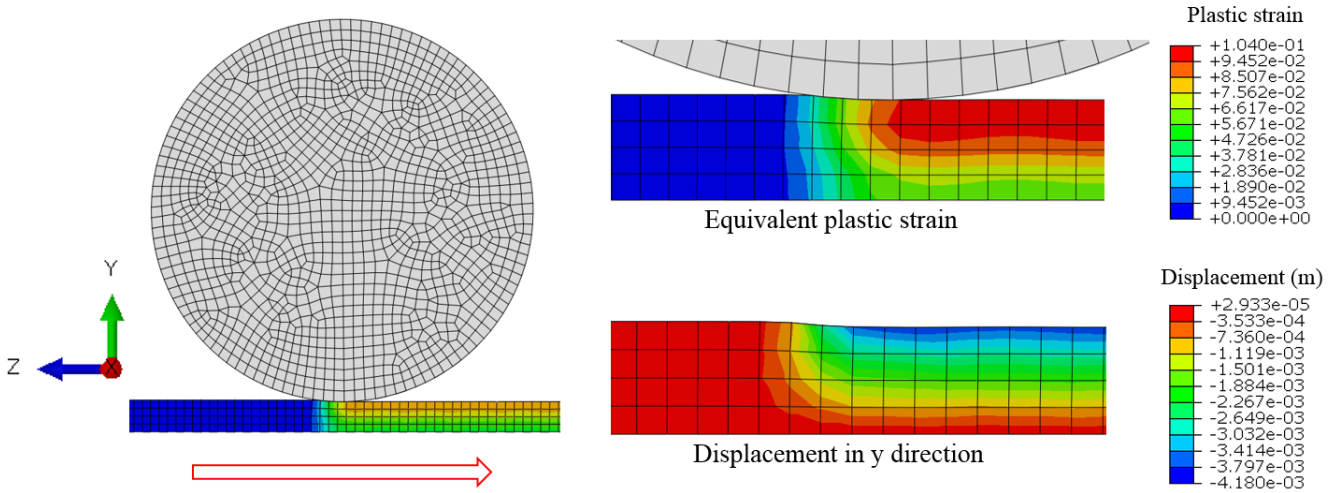

Figure 4. Plastic strain and displacement distribution in P1 of the plate rolling

Plate hot rolling - Accumulated plastic strain simulation

Finite element simulation was performed assuming strain accumulation between successive rolling passes to investigate mass flow behavior and the stress/strain accumulation during the plate hot rolling. In this simulation, it was assumed that recrystallization does not take place between passes, so residual stress and strain are fully accumulated from one pass to the next pass. The simulation results from P1 to P7 are shown in Figure 5. From P1 to P7, the plate surface continuously has larger plastic strain than the plate mid-thickness. The initial difference between the plate surface and mid-thickness at P1 is around 0.05, and this difference at P7 increases to 0.3 due to strain accumulation. The total strain at the plate surface at the end of P7 is almost 1, and the accumulated strain at the plate mid-thickness is around 0.7.

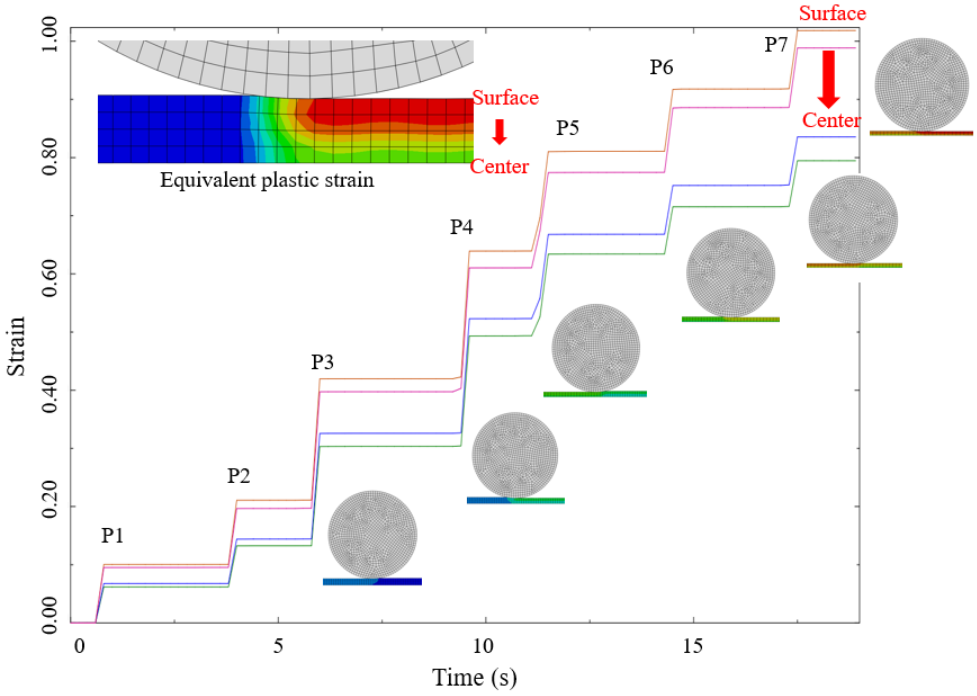

Figure 5. The accumulated simulation results of the plate rolling

Plate hot rolling – No accumulated plastic strain simulation

Finite element simulation was also performed to investigate the mass flow of each pass, assuming full recrystallization and no accumulation of residual stress and strain. The plastic strain distribution of each pass is similar to the results from the accumulated strain simulation. The plastic strain is larger at the plate surface than at the plate mid-thickness. For the no strain accumulation condition, the plastic strain differences between the plate surface and plate mid-thickness for each successive roll pass are comparable. The simulation results for each pass are shown in Figure 6. The maximum plastic strain determined for each pass indicates that P3-P5 have a largest deformation and the plastic strain is almost doubled compared to the other rolling passes. P3-P5 contribute more than 60% of the total deformation to the plate. The minimum plastic strain of each pass indicates that it is difficult to deform the slab center in P1, P2, P6, and P7 because of the smaller reductions employed for these passes. On the other hand, the plastic strain difference between the plate surface and mid-thickness increases only slightly as deformation increases. This difference is around 0.05 at P1, P2, P6, and P7 and is around 0.7 at P3-P5.

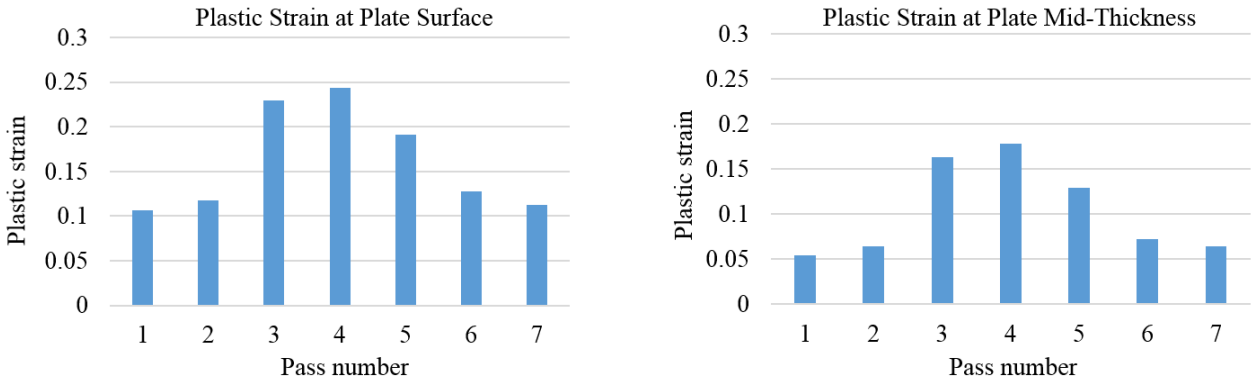

Figure 6. Maximum and minimum plastic strain of each pass

Simulation results for strip hot rolling

For the U. S. Steel hot strip mill, deformations imparted to the slab in the roughing stands were simulated. At the beginning of rolling, the slab goes through a vertical and a horizontal scale breaker, VSB and HSB, to remove scale developed during the reheat process. The slab is deformed by rollers and edgers after the scale breakers. At R1, no edger is included, while edgers are included for R2-R5. The function of edger is to control the slab width within a desired range. The function of the rollers in the roughing stand is to reduce the thickness of the slab prior to entering the finishing stands. Compared to the plate hot rolling at SSAB, the hot rolling at U. S. Steel is a continuous process. The rolling information is shown in Table 3.

Table 3. Typical rolling schedule of strip hot rolling

	R1	E1	R2	E2	R3	E3	R4	E4	R5
Diameter (inch)	49	33	49	33	43	33	43	33	43
Speed (fpm)	219	304	304	375	375	483	483	697	697
Gap (inch)	5.92	46.25	4.29	46.25	2.7	46.25	1.82	46.25	1.22

Strip hot rolling – Accumulated plastic strain simulation

An accumulated plastic strain simulation was performed for the U. S. Steel strip hot rolling. During this hot rolling, the mass flow behavior is different from the reversing rolling process. For example in plate hot rolling, the deformation is only vertical. In strip hot rolling, the deformations are both vertical from rolling and horizontal from the edger. The corresponding mass flow in the slab shows larger plastic strains on the edges than at the center (Figure 7).

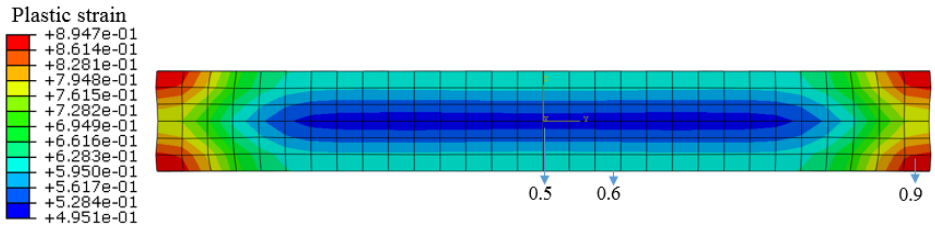

Figure 7. Mass flow behavior by both roller and edger

The accumulated strain simulation results are shown in Figure 8 where three nodes, node 1 on the edge, node 2 on the surface, and node 3 in the center are plotted. During VSB and HSB, slab was deformed slightly in the horizontal direction and vertical direction, respectively. From R1 to R5, node 1 on the edge always has larger plastic strain than the surface and center. Also, the effect of E1 to E4 is significant on the edge, while there is no effect on node 2 and node 3, indicating no deformation occurs in the center during E1 to E4. The simulation results show that edger has no effect on the center of slab, but it significantly changes the mass flow behavior at the edge.

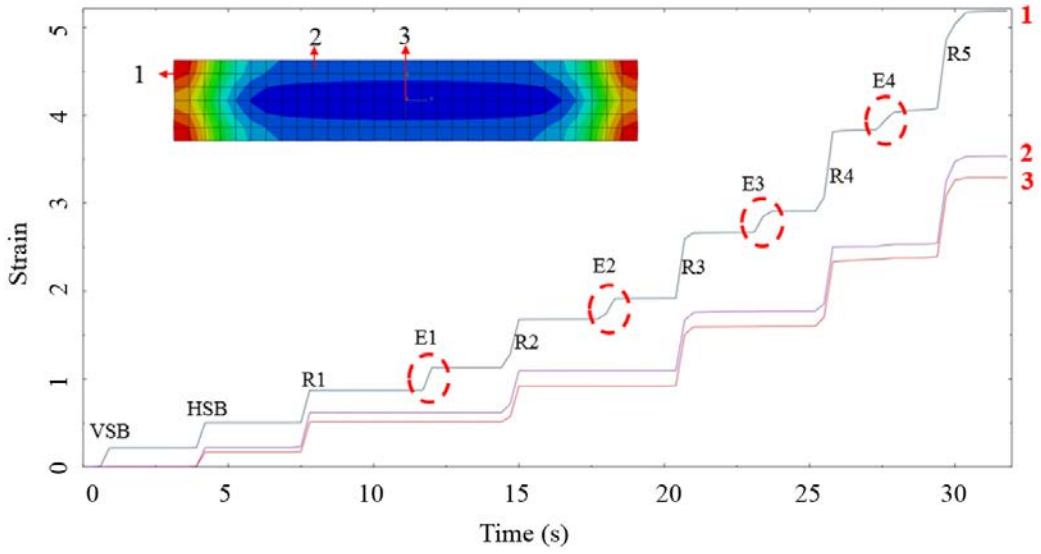

Figure 8. Accumulated plastic strain during strip hot rolling

Strip hot rolling – No accumulated plastic strain simulation

Finite element simulation was performed for the U. S. Steel strip hot rolling assuming no strain accumulation between rolling stands. The simulation results from R1 to R5 are shown in Figure 9. Since there was no edger before R1, the main deformation is on the top and bottom. The later passes R2-R5 have large deformation on the left and right edges of the slab. During edging, the material on the edge flows to the top and bottom surface. And during rolling, these edge areas have larger deformation than the center, resulting in large plastic strains in these areas.

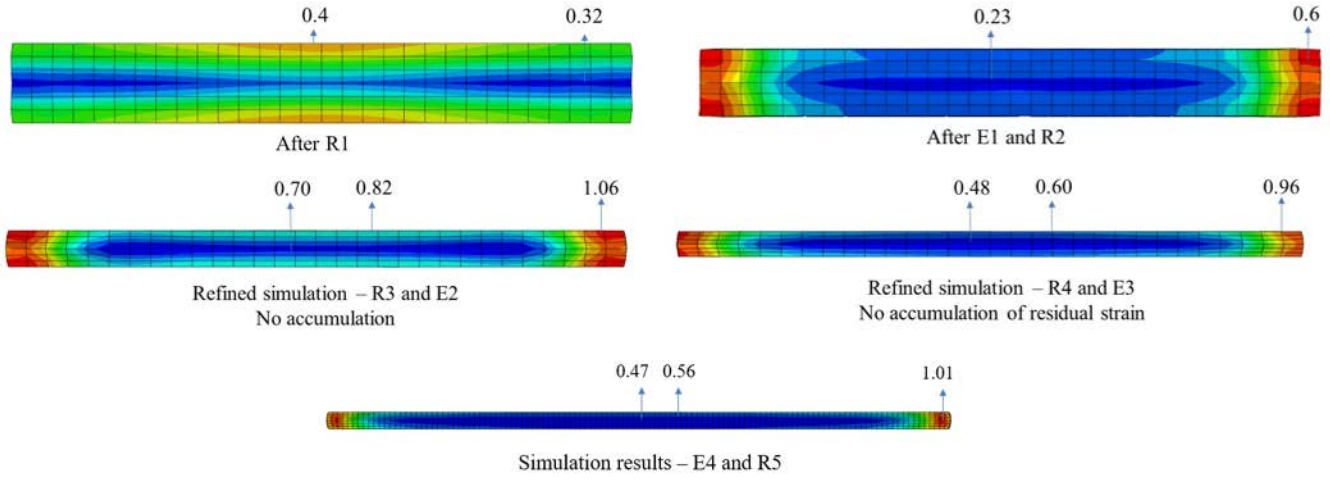

Figure 9. Simulation results of R1 to R5 of slab hot rolling

The detailed deformation of the edge, surface and center during hot rolling is shown in Figure 10. At R1, these three areas have similar plastic strain since no edger rolls are employed. Starting at R2, the maximum plastic strain is always at the edge. Also, R3 has larger deformation than the other passes, and R3-R5 have larger deformation than R1 and R2. The simulation results show that R1 has different mass flow compared to the other passes.

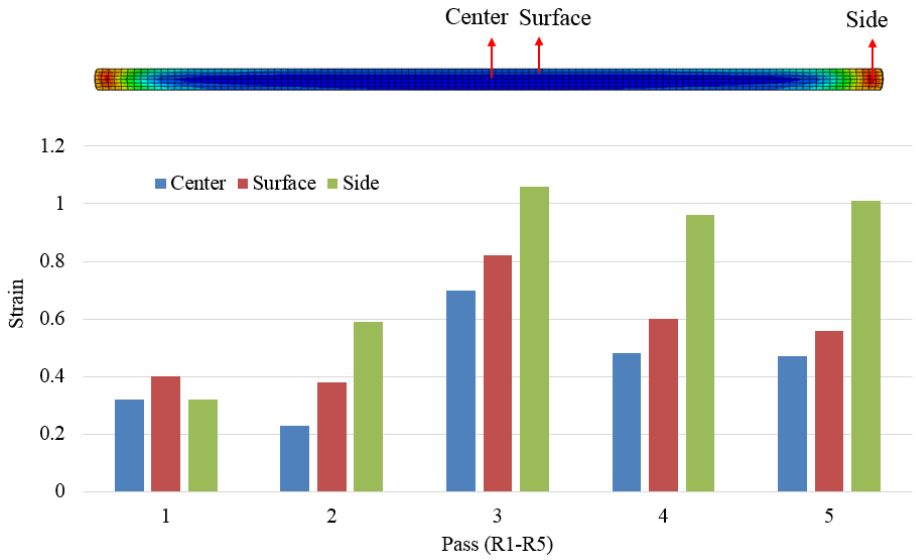

Figure 10. Comparison of plastic strain at each pass

Two different simulation approaches were used in this study to investigate industrial plate and strip hot rolling processes. The first approach assumed accumulated stress and strain during hot rolling process while the second approach supposed full recrystallization and recovery between rolling passes. Accumulated approach predicts material flow behavior while no accumulated approach was used to compare deformation between individual passes. In practice, strain accumulation during hot rolling will be between these two extreme cases. In this study, the proposed simulations can be used for quick assessment of industrial hot rolling schedules.

CONCLUSION

In this study, a three-dimensional nonlinear finite element model was developed for plate and slab hot rolling. Two Johnson-Cook models were developed and implemented into finite element models. For the SSAB plate hot rolling, a seven pass reversing rolling was modeled and simulated; for the U. S. Steel strip hot rolling, the multiple roughing stands with edgers were modeled and simulated. The mass flow behavior and plastic strain distribution were plotted and investigated. The simulation results show different mass flow behavior between the surface and center of plate and between the center and edge of the slab. It was demonstrated by the simulations that during the plate rolling, the plate surface has larger plastic strain than the center from P1 to P7. The deformation at P1, P2, P6, and P7 is small while the deformation at P3-P5 is doubled. The difference between surface and center of plate also increases as the deformation increases. During strip hot rolling, R1 shows different mass flow comparing with the other passes. The maximum plastic strain on R1 is on the top and bottom while the maximum plastic strain of the other passes occurs on the edge of slab due to edger. Also, the simulation results show that the deformation on R3-R5 is larger than R1 and R2.

ACKNOWLEDGEMENTS

This work is supported by the Peaslee Steel Manufacturing Research Center (PSMRC) at Missouri University of Science and Technology. The investigators acknowledge SSAB Americas and US Steel for supporting Hot Working Modeling and Simulation project.

DISCLAIMER

REFERENCES

[1] S. Kim and Y. Im, "Three-dimensional finite element analysis of non-isothermal shape rolling," *Journal of Materials Processing Technology*, vol. 127, pp. 57–63, 2002.

[2] X. Duan and T. Sheppard, "Three dimensional thermal mechanical coupled simulation during hot rolling of aluminium alloy 3003," *International Journal of Mechanical Sciences*, vol. 44, pp. 2155–2172, 2002.

[3] H. Ding, K. Hirai, T. Homma, and S. Kamado, "Numerical simulation for microstructure evolution in AM50 Mg alloy during hot rolling," *Computational Materials Science*, vol. 47, pp. 919–925, 2010.

[4] R. Mei, C. Li, X. Liu, and B. Han, "Analysis of strip temperature in hot rolling process by finite element method," *Journal of Iron and Steel Research International*, vol. 17, pp. 17–21, 2010.

[5] D. Benasciutti, E. Brusa, and G. Bazzaro, "Finite elements prediction of thermal stresses in work roll of hot rolling mills," *Procedia Engineering*, vol. 2, pp. 707–716, 2010.

[6] G. R. Johnson and W. H. Cook, "A constitutive model and data for metals subjected to large strains, high strain rates and high temperatures," *7th International Symposium on Ballistics*, vol. 21, pp. 541–547, 1983.

[7] F. J. Zerilli and R. W. Armstrong, "Dislocation-mechanics-based constitutive relations for material dynamics calculations," *Journal of Applied Physics*, vol. 61, pp. 1816–1825, 1987.

[8] S. Shida, "Empirical formula of flow stress of carbon steels—resistance to deformation of carbon steels at elevated temperature," *Journal of the Japan Society for Technology of Plasticity*, vol. 10, pp. 610–617, 1969.

[9] Y. Lin and X. Chen, "A critical review of experimental results and constitutive descriptions for metals and alloys in hot working," *Materials & Design*, vol. 32, pp. 1733–1759, 2011.

[10] S. Rummel, D. Van Aken, R. O'Malley, X. Wang, and K. Chandrashekhara, "High Strain Rate Hot Deformation of Steels: Measurement and Simulation," *Proceedings of the AIST Long and Forged Products Symposium*, pp. 1-10, 2015.